Accelerated Pharmacokinetic Map Determination for Dynamic Contrast Enhanced MRI using Frequency-Domain Based Tofts Model

Nithin N Vajuvalli, Krupa N Nayak and Sairam Geethanath

***Abstract*—Dynamic Contrast Enhanced Magnetic Resonance Imaging (DCE-MRI) is widely used in the diagnosis of cancer and is also a promising tool for monitoring tumor response to treatment. The Tofts model has become a standard for the analysis of DCE-MRI. The process of curve fitting employed in the Tofts equation to obtain the pharmacokinetic (PK) parameters is time-consuming for high resolution scans. Current work demonstrates a frequency-domain approach applied to the standard Tofts equation to speed-up the process of curve-fitting in order to obtain the pharmacokinetic parameters. The results obtained show that using the frequency domain approach, the process of curve fitting is computationally more efficient compared to the time-domain approach.**

I. Introduction

Dynamic contrast-enhanced magnetic resonance imaging (DCE-MRI) is a non-invasive quantitative method of investigating microvascular structure and function by tracking the pharmacokinetics of injected low-molecular weight contrast agents (CA) as they pass through the tumor vasculature [1]. It is widely used in the diagnosis of cancer and becoming a promising tool to monitor tumor response to treatment [2-7]. This technique involves serial acquisition of MR images of a tissue of interest; before, during and after the injection of CA [8]. Interaction of CA with hydrogen nuclei varies the T_1 and T_2 relaxation times thereby varying the tissue contrast [9].

Analysis of dynamic contrast-enhanced MRI (DCE MRI) aims to derive quantitative parameters that characterize permeability, blood volume, extracellular blood volume that provide very critical information about the tumor physiology by tracking the functional changes that occur in the tumor and play a very important role in clinical diagnosis, staging and treatment monitoring [8, 10-12].

Multiple pharmacokinetic models like the Tofts Model, Brix Model, Larsson Model, Hayton Model, [13-16] etc. have been proposed for the analysis of DCE-MRI images.

Dr. Sairam. Geethanath is with Dayananda Sagar College of Engineering, Bangalore, Karnataka, India (Phone: +919448293026; email: sairam.geethanath@dayanandasagar.edu)

Nithin N Vajuvalli is currently working as a Lecturer at Dayananda Sagar College of Engineering, Bangalore, Karnataka, India (email: nithinvajuvalli@gmail.com)

Krupa N Nayak is currently pursuing Master of Technology at Dayananda Sagar College of Engineering, Bangalore, Karnataka, India (email: krupannayak@gmail.com)

II. Theory

Tofts Model in Time-Domain (TD): Tofts model is an adaptation of the pharmacokinetic model for the measurement of blood brain barrier permeability proposed in [18]. It is a simplified model that considers the tissue of interest i.e., Extracellular Extravascular Space (EES) as one compartment and everything extraneous to it as another compartment (Plasma) and models the kinetics of the contrast agent as an exchange between the two [5].

The rates of the exchange of the CA between the two compartments are denoted by the PK parameters: K^{trans} (min^{-1}) and k_{ep} (min^{-1}). Here, K^{trans} quantifies the flow of CA from the plasma to the EES and k_{ep} quantifies the flow of CA from the EES to the plasma [4].

Tofts Model is explained using (1), where $C_a(t)$ is the Arterial Input Function (AIF) and represents the CA concentration in the plasma of a feeding artery(AU), C(t) is the concentration of CA in the EES and t is the time(sec). These parameters are measured quantities and are the known parameters in the equation.

$$C(t)=K^{trans} \exp(-k_{ep}t) \Theta C_a(t) \quad (1)$$

where, "Θ" is convolution. By fitting the DCE-MRI data to this model, the unknown PK parameters K^{trans} and k_{ep} can be extracted.

However, estimation of AIF plays a key role in obtaining the accurate parameter estimates of K^{trans} and k_{ep}[2-3]. The CA is injected intravenously as a bolus and once it reaches the vascular system, it is dispersed. It almost gradually washes out by the time it reaches the capillary system. Hence, it is not possible to measure the AIF directly in the capillary and is usually approximated. But when AIF is measured, it is sampled in an artery close to the tissue that is being imaged.

However, convolution becomes very tedious as the size of the image increases. Thus, the process of curve fitting slows down due to a large number of convolution computations. A new method is proposed to reduce the computation time for calculating the PK parameters by accelerating the process of curve-fitting

Tofts model in Frequency Domain (FD): The following equations describe the FD method employed in Tofts equation. According to the Convolution Theorem, a property of convolution of Fourier transforms; convolution in time domain is equivalent to multiplication in frequency domain. Hence, Fourier-transformed version of (1) is given as:

978-1-4244-7929-0/14/$26.00 ©2014 IEEE

$$\mathcal{F}\{C(t)\} = \mathcal{F}\{ K^{trans} \exp(-k_{ep}t)\} \; X \mathcal{F}\{C_a(t)\} \quad (2)$$

Replacing $\mathcal{F}\{C(t)\}=K_1$ and $\mathcal{F}\{C_a(t)\}=K_2$ and taking K_2 to the left hand side, the following equation is obtained:

$$(K_1/K_2) = K = \mathcal{F}\{ K^{trans} \exp(-k_{ep}t)\} \quad (3)$$

Taking inverse Fourier transform on both sides of (3),

$$\mathcal{F}^{-1}(K) = \mathcal{F}^{-1}(\mathcal{F}\{K^{trans}\exp(-k_{ep}t)\}) \quad (4)$$

Thus, the equation in its final form can be written as (5) which is used to find the kinetic parameters K^{trans} and k_{ep} through curve fitting.

$$\text{real}(\mathcal{F}^{-1}\{K\}) = \text{real}\{K^{trans}\exp(-k_{ep}t)\} \quad (5)$$

The above equation is independent of convolution making it simplified for computation. In other words, the computational complexity of convolution is replaced with the fast Fourier transform which reduces the number of computations performed, thus speeding up the entire process.

III. Methods

Previously acquired DCE data of breast tumor bearing rats was used for the experiment. The DCE data set had dimensions of 64x64 and consisted of 64 images acquired with temporal resolution of 12 seconds. This data set consisted of 4 pre-contrast images and 60 post-contrast images. Omniscan (0.1 mmol/kg) was intravenously administered through the tail vein.

Two methods were used for quantification of PK parameters from the DCE-MRI dataset: Tofts Model using TD approach and Tofts Model using FD approach. These methods were evaluated for reduction in computation time by generating random values of different matrix dimensions. These two methods were also applied to the DCE data of the breast-tumor bearing rats and the methods are compared by evaluating PK maps.

The Tofts Equation in (1) in TD consists of a convolution term, which is used to obtain PK parameters and (5) which is independent of convolution is used to obtain PK parameters in the FD method. The execution times for both methods were noted. Nonlinear Least Squares method is used along with the Trust-region algorithm for curve fitting the equations to obtain the PK values.

To test the accuracy of curve fitting, random values of K^{trans} and k_{ep} were forward simulated and validated through computation of Root Mean Square Error (RMSE) given by the following equation.

$$RMSE = \text{Sqrt}[\Sigma(A-B)^2/\text{Length}(A)] \quad (6)$$

For forward solving of the Tofts model, random values of K^{trans} and k_{ep} are generated. The values of $C_a(t)$ and t are assumed and the equation is solved for C(t) using (1). The randomly generated values of K^{trans} and k_{ep} are taken as the ground truth. Next, with same values of $C_a(t)$, t and the value of C(t) obtained is taken and the equation is curve fitted to obtain the values of K^{trans} and k_{ep}. A new set of values are obtained for K^{trans} and k_{ep} through curve fitting. The same procedure of first forward solving and the curve-fitting was followed for the proposed FD method as well. Finally the root mean square error (RMSE) is calculated for the randomly generated values of K^{trans} and k_{ep} and the obtained values of K^{trans} and k_{ep}. In (6) A is the randomly generated data and B is the value obtained through curve fitting. All the computations were performed using Matlab, Mathworks Inc., Boston, MA.

IV. Results

A set of baseline, wash-in and wash-out images were obtained the breast tumor bearing rats. The concentration maps(AU) at different time points are shown in Fig 1. The concentration map shown in Fig 1(a) represents the 19th frame which is obtained during the wash-in phase.

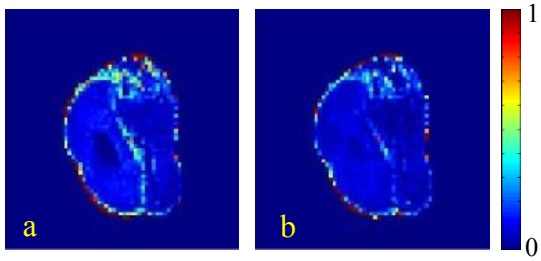

Figure 1. Concentration maps (AU) for: a: 19th frame b: 64th frame of a representative breast cancer data set

Fig 1(b) shows the wash-out phase of contrast agent in the 64th frame. It can be observed from the 19th frame that contrast enhancement has occured in this frame due to the injection of contrast agent and it appears brighter than the 64th frame in which the contrast agent has slowly started to exit.

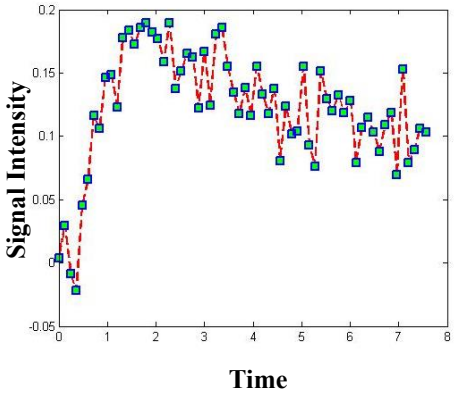

Figure 2. Arterial Input Function of a representative breast cancer dataset

Fig. 2 shows the AIF that was generated from the given data of 64 image frames which is used in the evaluation of Tofts model. The values that were obtained from the AIF shown in the figure was used in TD and FD calculations of the Tofts equation.

Fig 3(a) and Fig 3(b) show K^{trans} map and V_e map obtained by using the TD method of Tofts model. Fig 3(c) and Fig 3(d) show the K^{trans} and V_e map obtained using Tofts model in frequency domain.

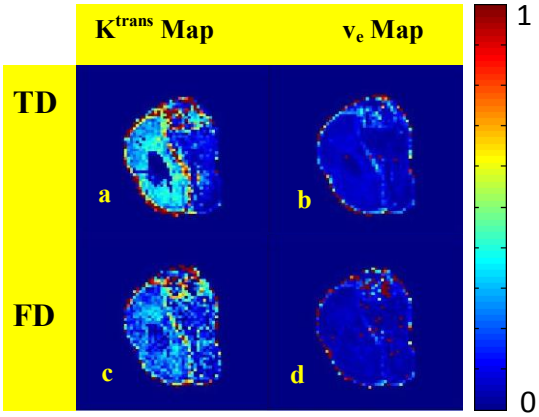

Figure 3. Pharmacokinetic Map of a representative breast cancer data set

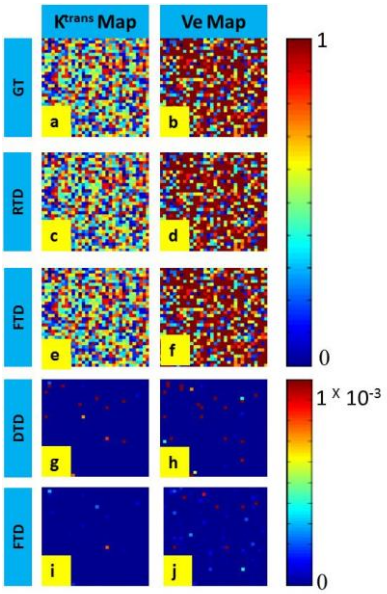

Figure 4. Pharmacokinetic Map of a representative randomly generated values along with differences between 2 methods

Fig 4a and Fig 4b shows the K^{trans} and V_e map for the randomly generated values, which is taken as the ground truth (GT) to compare two methods. Fig 4c and Fig 4d shows the K^{trans} and V_e map for the Reconstructed TD (RTD). Fig 4e and Fig 4f shows the K^{trans} and V_e map for the Reconstructed FD (RFD). Fig 4g and 4h shows the K^{trans} and V_e map Difference in TD (DTD) compared GT. Fig 4i and 4j shows the K^{trans} and V_e map Difference in FD (DFD) compared GT. It can be noticed that our RFD PK map had very small amount of error compared to the GT.

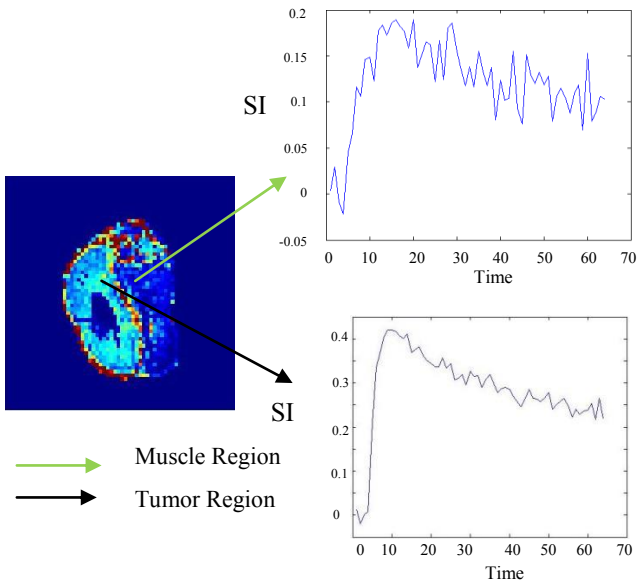

Figure 5. Typical relative enhancement curves for tumor and muscle region

It can be noticed from Fig. 5 that the signal intensity (SI) graph with time varies for the region of interest. The muscle region shows a gradual wash-in of the CA and it remains for a longer duration. Whereas, it can be observed in tumor region that there is a rapid wash-in of CA and it gradually wash-out.

Fig. 6 shows the graph of the time taken for computation of the PK parameters for the two methods for different matrix dimensions. It can be observed that the time taken for computation using FD method is less compared to the time taken for computation in TD method. The mean values of the time taken are plotted and it is noted that there is negligible standard deviation in both methods. A paired t-test was performed to compare our FD method with existing TD method for the obtained PK map and P value of 0.0002 was obtained and paring was significantly effective.

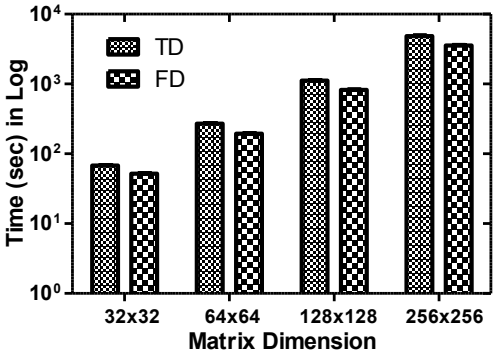

Figure 6. Graph of time taken for curve fitting using TD and FD

Fig. 7a and 7b show the graph for the mean K^{trans} & k_{ep} values respectively obtained for different matrix dimensions obtained using both methods. It can be observed from Fig. 6 that the mean of the RMSE values obtained randomly for different cases K^{trans} and k_{ep} obtained using curve fitting in frequency domain is lower when compared to the RMSE values obtained using curve fitting in time domain for randomly generated values.

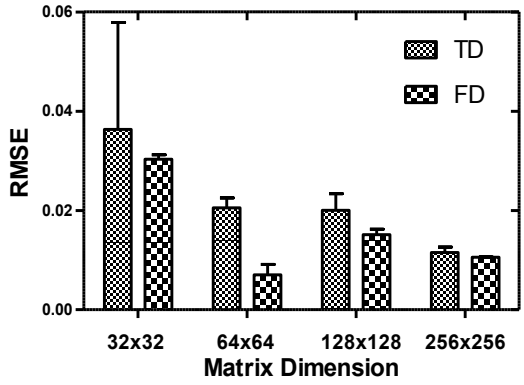

Figure 7a. Graph of RMSE values for K^{trans} the different matrix dimensions used in the two methods

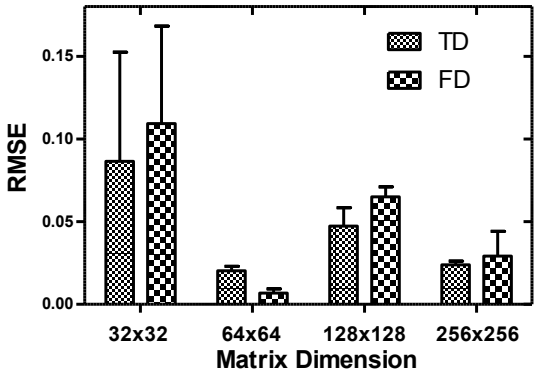

Figure 7b. Graph of RMSE values for k_{ep} the different matrix dimensions used in the two methods

V. CONCLUSION

The proposed FD method has efficiently reduced the processing time taken for curve fitting to generate the PK maps. Fast computation technique to generated parameter maps has been developed and successfully implemented on DCE data of a breast tumor bearing rats. RMSE values for Tofts Model using FD method was less when compared to the Tofts Model using TD method. Future work involves clinical and radiological evaluation to validate the method for diagnostic accuracy.

ACKNOWLEDGMENT

We would like to thank Vision Group of Science and Technology, TRIP grant 2013-14, for their support and Dr. Vikram Kodibagkar, ASU, for his support.

REFERENCES

[1] JPB O'Connor et al., "DCE-MRI biomarkers in the clinical evaluation of anti-angiogenic and vascular disrupting agents," *British Journal of Cancer* (2007) 96, pp. 189-195, Jan. 2007

[2] Roberta Fusco**, "**Lesion detection and classification in breast cancer: evaluation of approaches based on morphological features, tracer kinetic modelling and semi-quantitative parameters in MR functional imaging (DCE-MRI)," Ph.D. dissertation, Department of Biomedical Engineering, University of Bologna

[3] Anwar R. Padhani, "Dynamic Contrast –Enhanced MRI in Clinical Oncology: Current Status and Future Directions", *Journal of Magnetic Resonance Imaging*, 16:407-422, 2002

[4] Glenn Liu et al., "Dynamic Contrast-Enhanced Magnetic Resonance Imaging As a Pharmacodynamic Measure of Response After Acute Dosing of AG-013736, an Oral Angiogenesis Inhibitor, in Patients With Advanced Solid Tumors: Results From a Phase I Study," *Journal of Clinical Oncology*, Volume 23, Number 24, Aug 2005

[5] Roberta Fusco et al., "Dynamic contrast-enhanced MRI in breast cancer: A comparison between distributed and compartmental tracer kinetic models," *Journal of Biomedical Graphics and Computing*, ISSN 1925-4008, pp 23-36, Dec 2012

[6] Baris Turkbey et al., "The role of dynamic contrast enhanced MRI in cancer diagnosis and treatment," Diagn Interv Radiol 2010; 16:186–192, 2010

[7] Tofts P.S. et al.," Estimating kinetic parameters from dynamic contrast-enhanced T(1)-weighted MRI of a diffusable tracer: standardized quantities and symbols,"*J. Magnetic Resonance Imaging*," vol. 10, no. 3, pp. 223–232, Sep.1999

[8] Thomas E. Yankeelov et al., "Quantitative pharmacokinetic analysis of DCE-MRI data without an arterial input function: a reference region model," *Magnetic Resonance Imaging 23*, pp.519–529, Feb. 2005

[9] Anders Garpebring, "Contributions to Dynamic Contrast Enhanced MRI," Ph.D. dissertation, Department of Radiation Sciences, Radiation Physics, Umea University, 2011

[10] Carmel Hayes et al., "Assessing changes in tumor vascular function using Dynamic contrast enhanced magnetic resonance imaging," *NMR Biomed.* 2002;**15**:154–163

[11] Steven P. Sourbron et al, "On the Scope and Interpretation of the Tofts Models for DCE-MRI," *Magnetic Resonance in Medicine 66,* pp.735–745, Jan. 2011

[12] Alan Jackson et al., "Imaging tumor vascular heterogeneity and angiogenesis using dynamic contrast enhanced Magnetic Resonance Imaging," *Clin Cancer Res* 2007;13:3449-3459

[13] G. Brix, W. Semmler, R. Port, L. R. Schad, G. Layer, and W. J. Lorenz, "Pharmacokinetic parameters in CNS Gd-DTPA enhanced MR imaging," *Journal of Computer Assisted Tomography*, Vol. 15, pp. 621- 8, 1991.

[14] P. Hayton, M. Brady, L. Tarassenko, and N. Moore, "Analysis of dynamic MR breast images using a model of contrast enhancement," *Med Image Anal,* Vol. 1, pp. 207-24, 1997.

[15] H. B. Larsson, M. Stubgaard, J. L. Frederiksen, M. Jensen, O. Henriksen, and O. B. Paulson, "Quantitation of blood-brain barrier defect by magnetic resonance imaging and gadolinium-DTPA in patients with multiple sclerosis and brain tumors," *Magnetic Resonance Medicine,* Vol. 16, pp. 117-31, 1990.

[16] P. S. Tofts, B. Berkowitz, and M. D. Schnall, "Quantitative-analysis of dynamic Gd-DTPA enhancement in breast-tumors using a permeability model," *Magnetic Resonance in Medicine*, Vol. 33, pp. 564-568, 1995

[17] G.J.S. Litgens et al., "PharmacokineticModels in Clinical Practice: What model to use for DCE_MRI of the Breast?," ISBI 2010 IEEE 978-1-4244-4126-6/10 pp 185-188, 2010